Accepted Manuscript

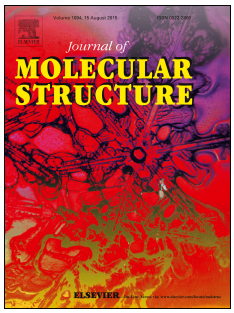

Synthesis, crystal structure, computational analysis and biological properties of 1-(4-chlorobenzoyl)-3-[2-(2-{2-[3-(4-chlorobenzoyl)-thioureido]-ethoxy}ethoxy)ethyl]-thiourea and its Ni(II) and Cu(II) complexes

Ebube Evaristus Oyeka, Jonnie Niyi Asegbeloyin, Ilknur Babahan, Bernard Eboma, Obinna Okpareke, Joseph Lane, Akachukwu Ibezim, H. Halil Bıyık, Bahadır Törün, David Chukwuma Izuogu

PII: S0022-2860(18)30571-4

DOI: 10.1016/j.molstruc.2018.05.015

Reference: MOLSTR 25187

To appear in: *Journal of Molecular Structure*

Received Date: 9 March 2018

Revised Date: 4 May 2018

Accepted Date: 5 May 2018

Please cite this article as: E.E. Oyeka, J.N. Asegbeloyin, I. Babahan, B. Eboma, O. Okpareke, J. Lane, A. Ibezim, H.H. Bıyık, Bahadı. Törün, D.C. Izuogu, Synthesis, crystal structure, computational analysis and biological properties of 1-(4-chlorobenzoyl)-3-[2-(2-{2-[3-(4-chlorobenzoyl)-thioureido]-ethoxy}ethoxy)ethyl]-thiourea and its Ni(II) and Cu(II) complexes, *Journal of Molecular Structure* (2018), doi: 10.1016/j.molstruc.2018.05.015.

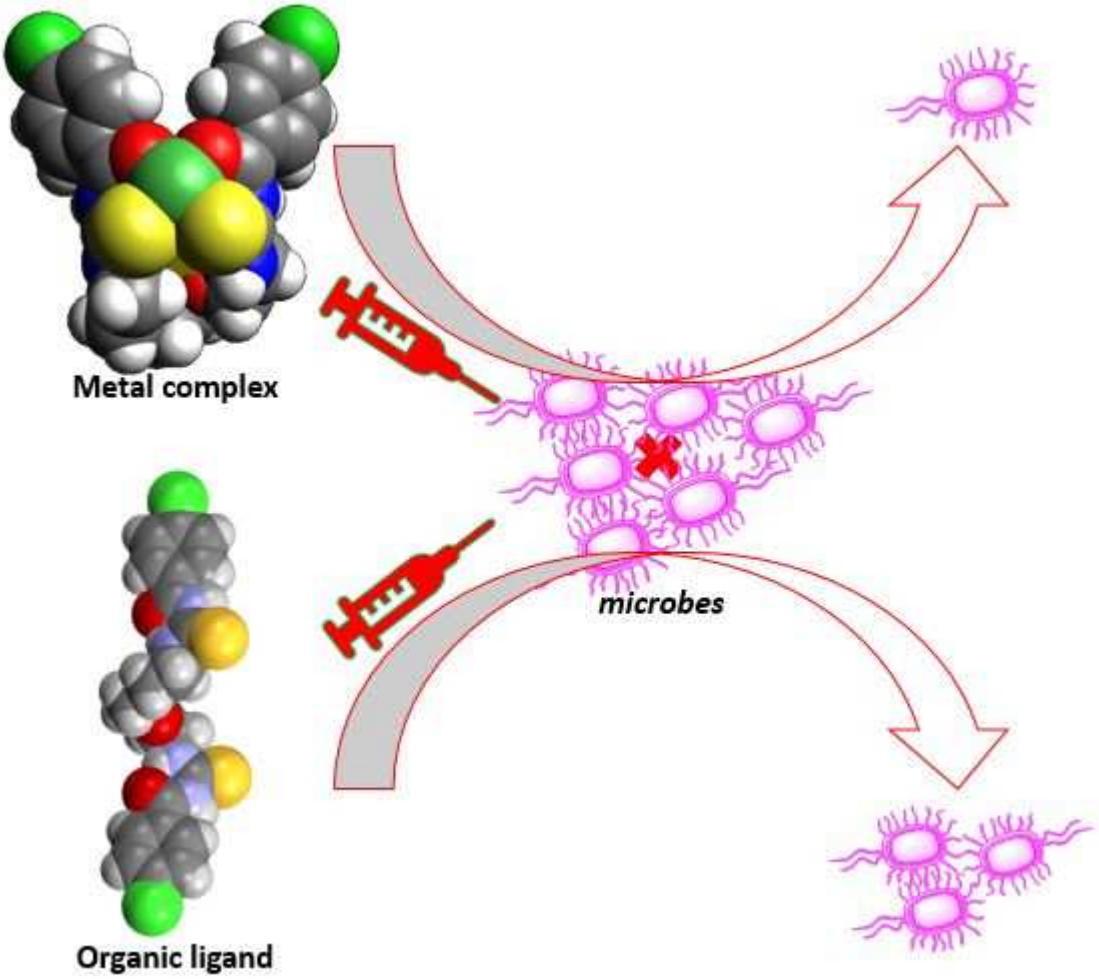

Synthesis, crystal structure, computational analysis and biological properties of 1-(4-chlorobenzoyl)-3-[2-(2-{2-[3-(4-chlorobenzoyl)-thioureido]-ethoxy}ethoxy)ethyl]-thiourea and its Ni(II) and Cu(II) complexes

Ebube Evaristus Oyeka[1,3], Jonnie Niyi Asegbeloyin[1*], Ilknur Babahan[2], Bernard Eboma[1], Obinna Okpareke[1,6], Joseph Lane[6], Akachukwu Ibezim[4], H. Halil Bıyık[5],Bahadır Törün[5] and David Chukwuma Izuogu[1,3],

[1]Department of Pure and Industrial Chemistry, University of Nigeria, Nsukka, Enugu State, Nigeria

[2] Department of Chemistry, Adnan Menderes University, 09010, Aydin, Turkey

[3] Department of Chemistry, Graduate School of Science, Tohoku University, 6-3 Aza-Aoba, Aoba-ku, Sendai, Miyagi, 980-8578 Japan

[4]Department of Pharmaceutical Chemistry, University of Nigeria, Nsukka, Enugu State, Nigeria

[5]Department of Biology, Adnan Menderes University, 09010, Aydin, Turkey

[6]School of Science, University of Waikato, Private Bag 3105, Hamilton, New Zealand.

Corresponding Author: niyi.asegbeloyin@unn.edu.ng

Abstract

A new dianionc ligand, 1-(4-chlorobenzoyl)-3-[2-(2-{2-[3-(4-chlorobenzoyl)-thioureido]-ethoxy}ethoxy)ethyl]-thiourea(CBEDEA), and its Ni(II) and Cu(II) complexes have been synthesized. X-ray single crystal analysis of CBEDEA shows that the molecule crystallized in the triclinic crystal system, space group P-1, with two molecules per unit cell. The studied compounds were further characterized by FT-IR, UV-VIS, ^{1}H NMR and mass spectroscopy. The metal complexes were isolated as four coordinated ML(M: Ni(II), Cu(II), L:CBEDEA) molecules. Computational studies on CBEDEA gave electrostatic potential energyisovalues which showed that there is a higher probability of metal coordination around the carbonyl and thione groups. Results of non-covalent interaction studies revealed the presence of significant amount of hydrogen bonding and other weak non-covalent interactions in the molecule. Docking calculations on CBEDEA and its Ni(II) and Cu(II) metal complexes revealed that they have affinity for beta-lactamase, a protein implicated in antibiotic drug-resistant mechanism. Complexation with the metal ion shrank the size of the molecule and enabled the metal complexes to fit more appropriately within the binding groove of the protein resulting in the improved affinity over CBEDEA ligand. Target-ligand binding interactions resulted from hydrophobicity and possibility of hydrogen bonding of the molecules. Furthermore, *in vitro* screening of the compounds against 17 bacteria and 4 yeasts confirmed their antimicrobial potency against more susceptible Gram-positive bacteria. Results of this study suggest that the metal complexes could be developed into novel antimicrobial compounds.

Keywords: Thiourea; Complexes; Spectroscopy; Computational; Docking calculations; Antimicrobial studies

1. Introduction

The coordination chemistry of thioureas and their derivatives have been the subject of investigations in recent times. Several works exploring the rich coordination geometries of this group of compounds have been reported in the literature[1-4]. Thiourea derivatives are versatile ligands with the ability to coordinate various metal centers in different coordination modes to form metal complexes with good stability [5]. The presence of hard O- and N- and soft S-donor atoms in the backbones of thioureas enable them to interact with both transition and main group metal ions, yielding metal complexes with interesting physicochemical properties and significant biological activities [1-2,4,6]. Thiourea derivatives can act as monodentate, bidentate or polydentate ligands, due to the presence of multi-donor atoms [7], and can coordinate a range of metal centres as neutral ligands [8], monoanions[3,4] or di-anions [9]. The introduction of carbonyl functional group to thiourea derivatives to give acylthiourea increases the binding ability of the compounds to both cations and anions [1], resulting in different levels of intramolecular and intermolecular hydrogen bonding interactions [10]. Thiourea functionalities are of great importance in supramolecular chemistry, owing to the strong hydrogen bond donor and acceptor ability of the N-H and C=S groups. They, therefore, take part in self-association processes such as dimer formation and binding to guest ions [11,12]. The hydrogen bonding ability of thiourea moieties has been utilized in the construction of anion receptors [13,14]. The high binding and ion receptive ability of thioureas are properties being exploited in their use as chemotherapeutics [15,16]. Higher hydrogen bonding interaction has been associated with increased target specificity to nuclear bases of DNA and oxidative cleavage of DNA, thereby enhancing anticancer activity [17]. A vast range of biological activities have been reported for acylthiourea derivatives which include antitumor [8,18], antibacterial [4,19,20], antifungal [21], herbicidal and insecticidal properties [4,19]. Also Ni(II) and Cu(II) complexes of thiourea derivatives have been reported to have appreciable biological activity [22,23].

The isolation of molecules suitable for x-ray studies has remained a challenge despite successes recorded in the past decades [24]. The design of molecular crystals involves proper understanding and control of the non-covalent interactions such as hydrogen bonding and Van der Waals forces which play significant roles in crystal formation. However, the utilization of thiourea functionality for building crystalline frameworks requires a different approach, so as to prevent them from self-association, and thereby make them available for binding guest ions [25]. Consequently, the use of quantum mechanical tools in the elucidation of effects such as non-covalent bond interactions and anion receptor properties in molecules is imperative.

Recently, we reported the crystal structure, computational and in-silico anticancer studies of N,N-diethyl-N'-palmitoylthiourea exhibiting strong intermolecular hydrogen bonding [26]. In the present

contribution, we have explored the synthesis, structure, non-covalent interaction and biological properties of a bis(acylthiourea) and its Ni(II) and Cu(II) complexes.

2. Experimental Methods

2.1. Chemicals and instrumentation

4-chlorobenzoylchloride, 2,2'-(ethylenedioxy)bis(ethylamine), acetone, dichloromethane, methanol, distilled water, potassium thiocyanate were obtained from Sigma Aldrich and used without further purification. Melting point was obtained with a Fisher John melting point apparatus. The infrared spectra were recorded in the range of 4000 – 400 cm^{-1} as KBr discs on a Perkin Elmer 100 Infrared Spectrophotometer. ^{1}H NMR spectra were obtained from a MERCURY-300 MHz NMR spectrometer using DMSO-D6 as a solvent. Mass spectra were obtained using a BruckerDaltonics ESI-MS spectrometer. The conductivity of the complexes was checked using a WTW LF90 conductivity meter by dipping the electrode of the meter into the solution of the sample and recording the reading at the National Centre for Energy Research and Development, University of Nigeria, Nsukka.

2.2. Synthesis of 1-(4-chlorobenzoyl)-3-[2-(2-{2-[3-(4-chlorobenzoyl)-thioureido]-ethoxy}ethoxy)ethyl]-thiourea (CBEDEA)

Synthesis of 1-(4-chlorobenzoyl)-3-[2-(2-{2-[3-(4-chlorobenzoyl)-thioureido]-ethoxy}ethoxy)ethyl]-thiourea (CBEDEA) was done by similar literature procedure [10].

A solution of 4-chlorobenzoylchloride (0.02 mol, 2.926 mL) in anhydrous acetone (40 mL) was added dropwise to a suspension of potassiumthiocyanate (0.02 mol, 1.944 g) in dry acetone (30 mL), and the reaction mixture was heated under reflux for 30 min and then cooled to room temperature. A solution of 2,2'-(ethylenedioxy)bis(ethylamine) (0.01 mol, 1.462 mL) in anhydrous acetone (30 mL) was added, and the resulting mixture stirred for 2 h. The solution was filtered to remove inorganic solid. The filtrate was left for few days and yellow solid was obtained. The solid was then washed with water and ethanol. Crystals suitable for X-ray crystallographic studies were obtained by dissolution followed by slow evaporation of the product in methanol/dichloromethane mixture 1:1 at room temperature for few days. Colour: yellow crystals; m.p: 164 ^{o}C, yield: 82 %, ES-MS : calculated 566.570 $[M+Na]^{+}$; experimental 566.1 $[M+Na]^{+}$; ^{1}H NMR (300 MHz, DMSO D_6): δ = 11.42 (s, 2H, NH), δ = 10.95 (s, 2H, NH), δ = 7.90 – 7.93 (d, 4H, Ar-H, J = 8.7 Hz), δ = 7.53 – 7.56 (d, 4H, Ar-H, J = 8.7 Hz), δ = 3.78-3.79 (t, 4H, CH_2-CH_2, J = 4.4 Hz), δ = 3.69 (t, 4H, -CH_2-O-, J = 6.5 Hz), δ = 3.62 (t, 4H, CH_2-NH-, J = 6.5 Hz); ^{13}C NMR (300 MHz, DMSO D_6): δ = 178.2 (C=O), 167.7 (C=S), δ = 30.5 – 135.7 (C-1 - C-22); IR (KBr): υ(cm^{-1}): 3411, 3243 (st, υN-H), 1667 (st, υC=O), 1261 (υC=S).

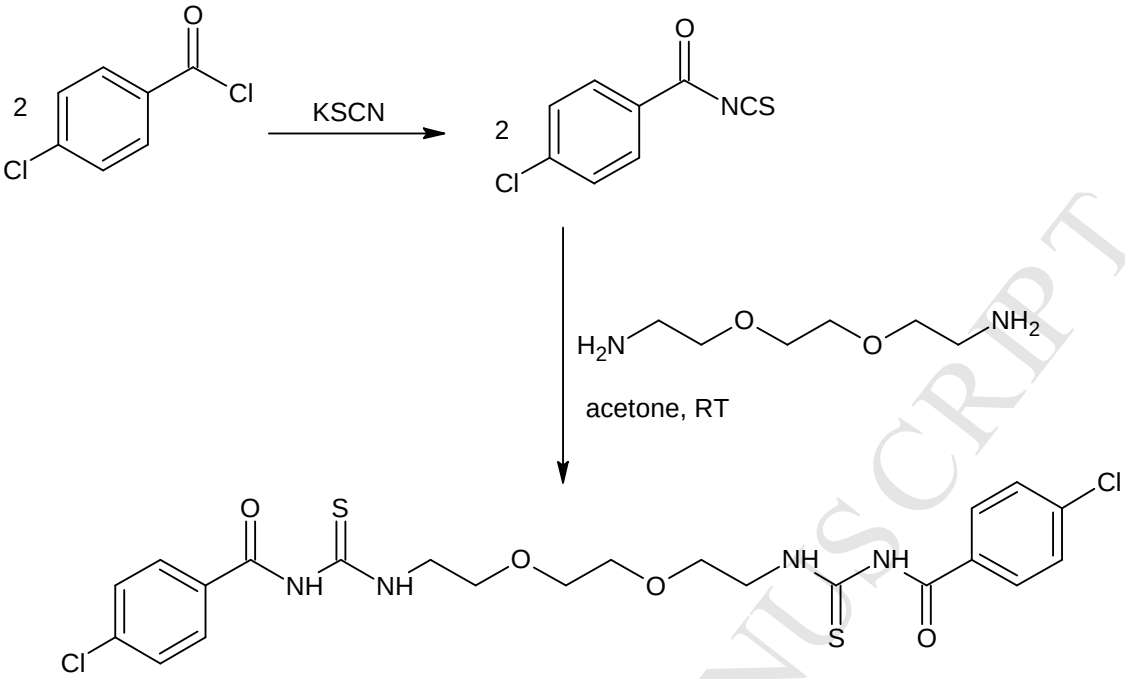

Scheme 1: Synthesis of 1-(4-chlorobenzoyl)-3-[2-(2-{2-[3-(4-chlorobenzoyl)-thioureido]-ethoxy}ethoxy)ethyl]-thiourea

2.3. Synthesis of Ni (II) complex of 1-(4-chlorobenzoyl)-3-[2-(2-{2-[3-(4-chlorobenzoyl)-thioureido]-ethoxy}ethoxy)ethyl]-thiourea (NiCBEDEA)

An ethanolic solution (20 ml) of $Ni(CH_3COOH)_2.4H_2O$ (1 mmol, 0.249 g) was added dropwise to a solution of 1-(4-chlorobenzoyl)-3-[2-(2-{2-[3-(4-chlorobenzoyl)-thioureido]-ethoxy}ethoxy)ethyl]-thiourea (1 mmol, 0.543 g) in ethanol (20 ml) at room temperature. The resulting mixture was stirred for 30 min at room temperature [27]. The solid complex formedwas filtered and recrystallized from methanol and dried in a dessicator. Colour: green; m.p: 212 ^oC; ES-MS : calculated 600.164 $[M]^+$; experimental 600.1 $[M]^{+1}$H NMR (300 MHz, $DMSOd_6$): δ = 10.97 (s, 2H, NH), δ = 7.92 (d, 4H, Ar-H), δ = 7.56 (d, 4H, Ar-H), δ = 3.77 (t, 4H, CH_2-CH_2), δ = 3.68 (t, 4H, -CH_2-O-), δ = 3.61 (t, 4H, CH_2-NH-); IR (KBr): υ(cm^{-1}): 3237 (st, υN-H), 1667 (st, υC=O), 1236 (υC=S), 1590 (υC=N).

2.4. Synthesis of Cu (II) complex of 1-(4-chlorobenzoyl)-3-[2-(2-{2-[3-(4-chlorobenzoyl)-thioureido]-ethoxy}ethoxy)ethyl]-thiourea (CuCBEDEA)

A solution of $CuCl_2.6H_2O$ (1 mmol, 0.171 g) in water (20 mL) was added dropwise to a solution of 1-(4-chlorobenzoyl)-3-[2-(2-{2-[3-(4-chlorobenzoyl)-thioureido]-ethoxy}ethoxy)ethyl]-thiourea (1 mmol, 0.543 g) in ethanol at room temperature. The resulting mixture was stirred for 30 min at room temperature [27]. The solid complex formed was filtered and recrystallized from methanol and dried in a dessicator. Colour: orange; m.p: 210 ^oC; ^1H NMR(300 MHz, $DMSOd_6$): δ = 11.30 (s, 2H, NH) δ = 7.92 (d, 4H, Ar-H), δ = 7.51 (d, 4H, Ar-H), δ = 3.2 - 3.55 (t, 12H, CH_2-CH_2, CH_2-O, CH_2-NH); IR (KBr): υ(cm^{-1}): 3171 (st, υN-H), 1634 (st, υC=O), 1255 (υC=S).

2.5. X-ray crystallography

The X-ray crystallographic data of 1-(4-chlorobenzoyl)-3-[2-(2-{2-[3-(4-chlorobenzoyl)-thioureido]-ethoxy}ethoxy)ethyl]-thioureawas obtained on a Bruker SMART APEX II diffractometer equipped with a CCD area detector using MoKα radiation (λ = 0.71073 Å). The software SMART was used for the collection of data frames, for indexing reflections, and to determine lattice parameters; SAINT was also used for the integration of the intensity of the reflections and for scaling. SADABS was used for empirical absorption correction. The structures were solved using SHELXS-97,which was also used for structure refinements and reporting. The structures were refined by full-matrix least-squares based on F_o^2 (SHELXL-97) with anisotropic thermal parameters for non-hydrogen atoms.

2.6. Computatonal studies

All theoretical calculations were performed using the Gaussian 09 program suite [28]on the high performance computing cluster at the University of Waikato. Initial input geometries were constructed from the crystal structure of CBEDEA. Geometry optimization was completed at the DFT level of theory with the ωB97XD density functional which includes empirical dispersion and the 6-311G+(2d,2p) basis set. This level of theory was found to have the highest congruency with the bond lengths and angles of the CBEDEA crystal structure. Quantum mechanical wave functions files were generated from the optimized structure of CBEDEA at the same level of theory. Non-covalent interaction (NCI) calculations were performed using the NCI index software [29].

2.7. Antimicrobial screening

2.7.1. Microorganisms and Condition for Cultivation

Seventeen bacteria and four yeast cultures were used in the study. The bacterial strains and three yeast strains were obtained from the American Type Culture Collection (ATCC, Rockville, MD, USA). *Candida trophicalis* were obtained from the Faculty of Medicine, Adnan Menderes University. The Gram-negative bacteria (G−) were *Escherichia coli* ATCC 35218, *Enterobacteraerogenes* ATCC 13048, *Salmonella typhimurium* ATCC 14028, *Klebsiellapneumoniae* ATCC 13882, *Pseudomonasaeruginosa* ATCC 35032, *Proteus vulgaris* ATCC 33420, *Serratiamarcescens*ATCC 13880, and the Gram-positive bacteria (G+) were *Micrococcus luteus* ATCC 9341, *Staphylococcus aureus* ATCC 25923, *Staphylococcus epidermidis* ATCC 12228, *Streptococcus pneumoniae* ATCC 27336, *Corynebacterium xerosis* ATCC 373, *Listeriamonocytogenes* ATCC 19112, *Enterococcus faecalis*ATCC29212, *Bacillus cereus* ATCC 11778, *Bacillus subtilis* ATCC 6633, Also, yeast strains such as *Candida utilis*ATCC 9950, *Candida albicans*ATCC 10231, *Candida tropicalis*, and *Saccharomyces cerevisiae* ATCC 9763 were used.

The bacterial strains were cultured in Tryptic Soy Agar (TSA) and Brain Heart Infusion Agar (BHIA) at 30-37 ^oC for 24 h. The yeast strains were cultured in Malt Extract Agar (MEA) at 30 ^oC for 24 h.

2.7.2. Antimicrobial Assay

The antimicrobial activities of all the synthesized compounds were determined by the discdiffusion method [30,31]and the minimum inhibitory concentrations (MIC) were obtained by broth dilution method [32-34].

2.7.3. Disc Diffusion method

The standard method of Antimicrobial Disc Susceptibility Tests reported by the National Committee for Clinical Laboratory Standards [30,31]was used. Fresh stock solutions (1000 $\mu g \cdot mL^{-1}$) of all the synthesized compounds were prepared in DMSO. The inoculum suspensions of the tested bacteria and yeasts were prepared from the broth cultures (18–24 h) and the turbidity equivalent adjusted to 0.5 McFarland standard tube to give a concentration of 1×10^8 bacterial cells/mL and 1×10^6 yeast cells/mL. To test the antimicrobial activity of all the synthesized compounds, a Mueller Hinton Agar (MHA) plate was inoculated with 0.1mL broth culture of bacteria or yeast. Then a hole of 6 mm in diameter and depth was made on top with a sterile stick and filled with 50 μL of synthesized compounds. Plates inoculated with *E. coli* ATCC 35218, *E. aerogenes* ATCC 13048, *S. typhimurium* ATCC 14028, *S. aureus* ATCC 25923, *S. epidermidis* ATCC 12228, *E. faecalis*ATCC 29212, *K. pneumoniae* ATCC13882, *P. Aeruginosa* ATCC 35032, *P. vulgaris* ATCC 33420, *S. arcescens*ATCC 13880, *S. pneumonia* ATCC 27336, *C. xerosis* ATCC 373 and *L. monocytogenes* ATCC 19112 were incubated at 37 ^oC for 24 h,while those with *M. luteus*ATCC 9341, *B. subtilis*ATCC 6633 and *B. cereus* ATCC 11778 were incubated at 30 ^oC for 24 h. In addition, *C. albicans*ATCC 10231, *C. utilis*ATCC 9950, *C. tropicalis*, and *S. cerevisiae* ATCC 9763 were incubated at 27◦C for 24 h. At the end of incubation time, the diameters of the inhibition zones formed on the MHA were evaluated in millimeters. Discs containing Chloramphenicol (30 mg Oxoid), Gentamycin (10 mg Oxoid), Tetracycline (30 mg Oxoid), Ampicillin (10 mg Oxoid), Ofloxacin (5 mg Oxoid), Vancomycin (30 mg Oxoid), Cefotaxime (30 mg Oxoid), Nystatin (100 mg Oxoid) were used as positive controls. The measured inhibition zones of the study compounds were compared with those of the reference discs.

2.7.4.Minimum Inhibitory Concentration (MIC)

Minimum inhibitory concentration (MIC) was determined by reported method[32-34].The study bacteria were inoculated in Tryptic Soy Broth (TSB) and Brain Heart Infusion Broth (BHIB) and incubated at 30–37 ◦C for 24 h while the yeasts were inoculated in Malt Extract Broth (MEB) and incubated at 27 ◦C for 24 h. The inoculums were adjusted according to 0.5 McFarland standard tubes. Initially, 100 μL of Mueller Hinton Broth (MHB) was placed in each well. After, the compounds were dissolved in DMSO (2 $mgmL^{-1}$) and transferred into the first well. Two fold serial dilutions of the compounds were carried out to determine the MIC, within the concentration range 256 to 0.125 μgmL^{-1}. Cultures were grown at 30–37 ◦C (18–20 h) and the final inoculum was approximately 10^6 $cfumL^{-1}$.The lowest concentration of the study compounds that resulted in complete inhibition of the

microorganisms was represented as MIC (μgmL^{-1}). Similar procedure was done on positive controls. In each case, the test was performed in triplicate and the results were expressed as means.

2.8. Molecular Simulations

X-ray crystal structures of beta lactamase co-crystallized with its inhibitor were retrieved from the protein databank (PDB code 1ONH) [35]. The protein-ligand complex dimers were treated as described in our earlier work [36] using Molecular Operating Environment (MOE) software running on Linux workstation. The three-dimensional chemical structure of CBEDEA and its metal (copper and nickel) complexes were generated using the graphical user interface of MOE. The proteins and ligands were energy minimized in Gromacs 4.2.2 using ffG53a6 [37]. The Auto Dock Tool implemented in AutoDock4.2 software was used to carry out docking after the docking protocol has been validated though the root mean square deviation method. A grid box size of 16 x 22 x 20 Å^3 points (spacing between the grid points of 0.375 A) was used which centered on the mass center (18.611, 21.867, 6.326) of the crystallographic macromolecule encompassing all active site atoms.

3. Results and discussion

3.1. Physical properties of the synthesized compounds

The ligand and metal complexes were isolated by recrystallization using suitable solvents. CBEDEA was sparingly soluble in water, it was soluble in polar organic solvents such ethanol, methanol and DMF and but highly soluble in dichloromethane and DMSO. The metal complexes are colored, non-hygroscopic and stable solids. They were soluble in ethanol, methanol, dichloromethane, DMSO and DMF, however they showed only slight solubility in water and diethylether. The low molar conductivity values of the complexes indicate that they are non-electrolytes. All the compounds showed satisfactory mass spectroscopic results. The data from the mass spectra are all in agreement with the expected molecular masses of the ligand and metal complexes. Some physical parameters of the synthesized compounds are shown in Table 1.

Table 1: Some Physical Parameters of the compounds

Compound	Colour	% yield	Melting point ^{o}C	M^{+} (Calculated)	ES-MS: $[M+Na]^{+}$ (Experimental)	Molar formular	Molar conductivity ($ohm^{-1}mol^{-1}cm^{-2}$)
CBEDEA	Yellow	82	164	543.486	566.1	$C_{22}H_{24}Cl_2N_4O_4S_2$	-
NiCBEDEA	Green	78	212	600.164	623.1	$C_{22}H_{22}Cl_2N_4NiO_4S_2$	0.87
CuCBEDEA	Orange	81	210	641.047	664.3	$C_{22}H_{26}Cl_2CuN_4O_6S_2$	0.98

3.2. Structural analysis of CBEDEA

The molecular structure and crystal packing of CBEDEA are shown in Figure 1 and 2 respectively. Table 2 gives the crystal data and structure refinement. The bond lengths and bond angles are listed in Table 3. The single x-ray structural analysis shows that CBEDEA crystallized in the triclinic crystal system with space group P-1 and Z = 2. The molecule possesses a zigzag shape enacted by the N3-C14-C13-O3 and N2-C9-C10-O2 torsion angles of 61.93 ^{o} and 65.98 ^{o} respectively. Also the chlorophenyl groups are *trans* to each other. The molecule is non-planar in relation to the carbonyl and thione carbons as can be seen from C17-C16-N4-C15, O1-C7-N1-C8, C1-C7-N1-C8 and O4-C16-N4-C15 dihedral angles of 172.04^{o}, -4.19^{o}, 174.70^{o} and -176.21^{o}. However, the acylthiourea group of the C1-C6 ring is more twisted than that of the C17-C22 ring.

The C16-O4, C15-S1, C7-O1 and C8-S2 bonds show typical double bond lengths of 1.227(2) Å, 1.666(2) Å, 1.224(2) Å and 1.670(2) Å respectively [20,38]. The C-N bonds in the vicinity of carbonyl and thione carbon, C16-N4 (1.372(2) Å), C15-N4 (1.395(2) Å), C15-N3 (1.319(3) Å), C8-N2 (1.320(2) Å), C8-N1 (1.392(3) Å) and C7-N1 (1.371(3) Å) are less than expected for an average C-N bond length of 1.48 Å, therefore showing different degrees of double bond character [20,39]. This can be explained as resulting from the contribution of the thiol tautomer formed by the conjugation of the C=S π-electrons with the lone pairs of electrons on nitrogen. The shortening of the C-N bonds between the aliphatic substituent and the thione carbon, C15-N3 (1.319(3) Å) and C8-N2 (1.320(2) Å) compare to other C-N bonds in the molecule are in agreement with literature reports for other acylthiourea derivatives [20,26,38,39,40]. The C-C, C-O and C-N bonds of the 2,2'-(ethylenedioxy)bis(ethylamine) moiety are close to values expected for average single bond length of aliphatic systems; C-C (1.54 Å), C-O (1.43 Å), C-N (1.48 Å).The C-C bond, C11-C12 (1.492(3) Å), C10-C9 (1.499(3) Å), C13-C14 (1.496(3) Å) are slightly shorter because of the influence of the electronegative oxygen. The two 4-chlorobenzoylthiourea moieties of CBEDEA are expected to be equivalent, they, however, possess different bond lengths and bond angles as can be seen in Table 2. The bond angles of the 2,2'-(ethylenedioxy)bis(ethylamine) chain C11-O2-C10 (112.22^{o}), C13-O3-C12 (112.21 ^{o}), C14-C13-O3 (108.41 ^{o}), C11-C12-O3 (109.31 ^{o}) show single bond character with sp^3 hybridization, while those of

the phenyl ring, carbonyl and thione moieties are essentially sp^2 hybridized. The geometry of the carbonyl and thiocarbonyl groups each of the acylthiourea moiety is planar.

The CBEDEA molecule is stabilized by two equivalent intramolecular hydrogen bonds through N2-H2···O1 and N3-H3···O4. The thione group was not involved in any hydrogen bonding. No intermolecular hydrogen bond was observed in the molecule. Thus, CBEDEA is expected to show an excellent binding ability for guest ions because of the presence of free hydrogen bond donor and acceptor groups.

Table 2: Crystal data and structure refinement details for CBEDEA

Identification Code	**CBEDEA**
Formula	$C_{22}H_{24}Cl_2N_4O_4S_2$
Formula weight	543.47
Temperature (K)	100(2)
Wavelength (Å)	0.71073
Crystal system	Triclinic
Space group	P-1
a/Å	7.6280(4)
b/Å	9.1780(5)
c/Å	18.1787(10)
α/°	77.754(3)
β/°	86.591(3)
γ/°	79.544(3)
Volume (Å^3)	1222.78(12)
Z	2
Calculated density (g/cm^3)	1.476
Absorption coefficient (mm^{-1})	0.474
F(000)	564.0
Crystal size (mm^3)	0.604 × 0.362 × 0.285
Index	-9<=h<=9, -10<=k<=10, -21<=l<=21
Theta range for data collection	2.293 to 25.043
Reflections collected / independent reflections	17703/ 4316 [R(int) = 0.0359]
Completeness to theta (%)	99.9
Absorption correction	SADABS
Largest diff. peak and hole	0.284 and -0.208 e.Å^{-3}
Refinement method	Full-matrix least square on F^2
Goodness of fit on F^2	1.046
Final *R* indices [I>2σ(I)]	*R1* = 0.0321, *wR2* = 0.0747
R indices (all data)	*R1* = 0.0412, *wR2* = 0.0797

Table 3: Bond lengths (Å) and bond angles (^{o})

Bond Lengths			
Cl1 C4	1.734(2)	C11 O2	1.427(2)
C5 C6	1.378(3)	C12 O3	1.424(3)
C1 C7	1.492(3)	C13 O3	1.418(2)
C7 O1	1.224(2)	C13 C14	1.496(3)
C7 N1	1.371(3)	C14 N3	1.451(2)
C8 N1	1.392(3)	C15 N3	1.319(3)
C8 S2	1.670(2)	C15 N4	1.395(2)
C8 N2	1.320(2)	C16 N4	1.372(2)
C9 N2	1.456(2)	C16 O4	1.227(2)
C10 O2	1.419(2)	C17 C22	1.389(3)
C15 S1	1.666(2)	N3 H3	0.8800
Bond Angles			
C6 C1 C7	123.75(18)	N3 C15 N4	117.02(17)
H3A C2 C3	119.5	N3 C15 S1	123.78(15)
C3 C4 Cl1	120.38(17)	N4 C15 S1	119.17(15)
C4 C5 C6	119.36(19)	C17 C16 O4	120.42(17)
C1 C7 N1	116.79(17)	N4 C16 O4	122.02(18)
N1 C7 O1	121.22(18)	C16 C17 C22	124.85(17)
N1 C8 N2	116.70(18)	C7 N1 C8	128.28(17)
N1 C8 S2	118.58(15)	C8 N2 C9	122.56(17)
N2 C8 S2	124.72(16)	C8 N2 H2	118.7
C9 C10 O2	107.01(16)	C10 O2 C11	112.21(14)

3.3. Spectroscopic analysis of CBEDEA

In the ^{1}H NMR spectra of CBEDEA, there were characteristic peaks in the aliphatic, aromatic and hydrogen bonded regions. The triplet peaks at δ3.62 and δ3.69 were assigned to the CH_2-N and CH_2-O protons. The -CH_2-CH_2- protons were assigned to the triplet band at δ3.79. The doublets at δ7.73-7.93 were assigned to the aromatic protons of the 4-chlorophenyl, while the characteristic NH protons appeared at δ10.95 and δ 11.42. The δ11.42 band was explicitly assigned to the NH adjacent to the C=S group because of its involvement in N-H···O intramolecular hydrogen bonding as affirmed by the x-ray crystallographic analysis.

In the FTIR spectra of CBEDEA, the sharp and strong band at 3411 and 3242 cm^{-1} were ascribed to the stretching vibration of the N-H groups. This agrees with the report from the ^{1}H NMR spectra. The C=O stretching vibration was assigned to a strong absorption peak at 1667 cm^{-1}, which is in agreement with the literature reports [4,10,20,41]. A sharp absorption band with weak intensity observed at 1261 cm^{-1} was assigned to C=S stretching vibration [4,20,41]. The characteristic C-H stretch of aliphatic groups is expected to appear in 2850-3000 cm^{-1} frequency range and this was observed for CBEDEA at 2872 cm^{-1}. Aromatic C-H stretch was observed at 2931 cm^{-1}. The C-N stretching vibration could not be assigned because it appeared in the fingerprint zone of the IR. All the peaks observed in the IR spectra of CBEDEA were consistent with the results from the NMR spectra and X-crystallography and were also in good agreement with related literature spectra[4,10,20,41]. The UV spectra for CBEDEA was recorded in ethanol solution and an absorption band was observed at 235 nm which is due to the $\pi^{*}\leftarrow$n electronic transition of the C=S bond.

The ESI mass spectra of CBEDEA, CuCBEDEA and NiCBEDEA showed parent peak at 566.10, 623.1 and 664.3 respectively for $[M+Na]^{+}$, and this values are is in close agreement with calculated values. In the spectra of CBEDEA, adjacent peaks appeared at 567.10 and 568.10 which are due to contribution of the isotopic carbon-13 and chlorine-37 respectively. The detailed mass fragmentation patterns of the synthesized compounds can be found in the supplementary information.

3.4. Electrostatic Potential Energy

The strength of nearby charges, nuclei and electrons at any given position (equation 1) can be ascertained by measuring the electrostatic potential (ESP) energy,

$$\int_{\infty}^{D_f} K\frac{q_1 q_2}{r} \qquad 1.$$

K= Coulomb's constant q = charge of particles and r = separation between particles or radius.

Electrostatic potential maps or potential energy surface maps are electron density models used in theoretical chemistry to represent areas of high or low potential energy in a molecule. They are three-dimensional representations of the charge distribution of a molecule and thus an indication of the potential energy distribution of that molecule [42]. Areas of low potential are mapped in red and

characterized by an abundance of electrons while areas of high potential are mapped in blue and characterized by a relative absence of electrons (Figure 3). The regions of intermediary electron distribution are mapped from yellow to green. The ESP map gives an indication of the polarity or dipole moment of a molecule and this information can be used in predicting the chemical reactivity of the molecule of interest towards other molecules. In the case of the CBEDEA ligand, the ESP and its contour diagram (Figure 3a and 3b respectively) indicate the possible coordination sites of the ligand to metal ions. The electrostatic potential map for CBEDEA was generated from the optimized structure of the molecule at DFT level of theory using the Self Consistent Field (SCF) density matrix. The highest electronegative point of the molecule with the most intense red color was observed to be around the two carbonyl oxygens with an electrostatic potential isovalue of -0.045 and the most electropositive point on the molecule with the most intense blue coloration were observed to be around the phenyl rings with electrostatic potential isovalue of +0.471. The ESP maps show that there is a higher probability of metal coordination around the carbonyl and thione functional groups of the CBEDEA ligand than any other part of the molecule.

3.5. Analysis of Non-covalent interaction calculations

A wide range of interactions including hydrogen bonding, dispersion forces, Pauli repulsion, dipole-dipole attraction, CH---π, CH…..lone pair and lone pair ….π have recently been classified as non-covalent interactions [43]. Among these interactions, hydrogen bonding isthe most ubiquitous. The nature and strength of the different non-covalent interactions in a molecule determine the supramolecular architecture of the compound in the solid state. The relatively recently developed non-covalent interaction index (NCI index) [29] has been used to visualize real space regions where non-covalent interactions are located. The NCI index depends on the analysis and pictorial interpretation of the electron density (ρ) and its derivatives which includes the Hessian eigen value λ_2 and its reduced density gradient(s) which has been defined as

$$s = \frac{1}{2(3\pi^2)^{1/3}} \frac{|\nabla\rho|}{\rho(\mathbf{r})^{4/3}} \qquad 2.$$

Non-covalent interactions can be identified as regions in three-dimensional space where the reduced density gradient (s) and the electron density ρ are tending to zero [43]. The NCI index plots the reduced gradient as a function of the electron density ρ, oriented by the sign λ_2 which identifies the interaction types. Attractive interactions appear at $\lambda < 0$ while repulsive interactions appear at $\lambda > 0$ (as in the centre of rings or cages) where several non-bonded atoms interact resulting in steric crowding [44]. Pictorial 3D representation of these interactions in an RGB (red-green-blue) colouring scheme is used to rank these interactions. Red is used for repulsive/destabilizing interactions, blue for attractive/stabilizing interactions and green for delocalized weak interactions. The 2D electron density plots for CBEDEA and the corresponding 3D isosurface representations are shown in Figure 4. The low density, low gradient peak at $\text{sign}(\lambda_2)\rho < -0.03$ au is characteristic of an attractive intramolecular hydrogen bonding interaction on two ends of the CBEDEA molecule and corresponding to the deep blue end of the trophy

shaped bicolored isosurface trough between the thiourea N----H and the adjacent carbonyl C=O functional group. The red lower end of the isosurface trough corresponds to the low gradient high density peaks appearing at 0.01 au > sign(λ_2)ρ < 0.02 au. This is as a result of non-bondingmulticentric ring closure interactions in the six membered ring resulting from the intramolecular hydrogen bonding interaction. The other high density low gradient peaks appearing at sign(λ_2)ρ > 0.02 au are as a result of the non-bonding steric interactions within the benzene rings on each side of the CBEDEA ligand. This interaction corresponds to the deep red cigarshaped isosurface troughs situated at the center of the benzene rings. Apart from the hydrogen bonding interactions and the destabilizing steric interactions, the other type of interactions present in the solid state structure of the CBEDEA ligand are the CH----O=C intramolecular interactions, the weak CH---S=C intramolecular interactions, and the very weak CH----HN delocalized Van der Waals interactions. The low gradient low density peak for the attractive intramolecularCH----O=C interactions appear at sign(λ_2)ρ = 0.015 au on the 2D electron density plot. This corresponds to the blue end of the flat bicolored isosurface inside the five membered ring formed by the intramolecular CH----O=C interaction. The red end of the flat isosurface trough corressponds to the electron density peaks at 0.01 au > sign(λ_2)ρ < 0.02 au resulting from multicentric ring closure interactions. Similar multicentric ring closure interactions have been reported for intra-molecular CH----O=C interactions in N-acetyl phenylalanyl-amide [45]. The low density low gradient peaks at -0.01 au > sign(λ_2)ρ < -0.012 au are as a result of the weakly attractive intramolecular CH---S=C interactions corresponding to the light blue end of the flat isosurface troughs between the thio-carbonyl functional group and the adjacent phenyl carbon as shown on 3D isosurface plot in Figure 4. The orange coloured end of the flat isosurface corresponding to the almost simultaneous critical density value 0.01 au < sign(λ_2)ρ < 0.012 au are as a result of the strain on the ring back bone resulting from non-bonding multicentric interactions within the ring. This type of simultaneous interactions was also reported in the solid state structure of a related *N,N*-diethyl-N'-palmitoylthiourea[26]. The CH----NH delocalized interactions have been known to appear at critical density values of -0.01 au > sign(λ_2)ρ < 0.01 au and the two simultaneous critical density peaks within this range on the 2D density plots have been assigned to weak delocalized VanderWaal interactions in the CBEDEA ligand.The large amount of hydrogen bonding and other weak non-covalent interaction in the molecule is a pointer to the possibility of a high degree of bioactivity for the CBEDEA ligand.

3.6. Spectroscopic analysis of the metal complexes

The ^{1}H NMR of the diamagnetic nickel complex NiCBEDEA showed the disappearance of two protons at δ11.42 ppm which were assigned to the NH protons between the thione and carbonyl groups. This shows that there is deprotonation on metal chelation. The other peaks of the metal complexes shifted only slightly from the corresponding peaks in the ligand spectra.

The IR peak at 3411 cm^{-1} which was assignable to the N-H in the vicinity of the thione and the carbonyl group disappeared in the copper complex while that at 3243 cm^{-1} was shifted to a lower frequency. This is as a result of deprotonation of the N-H proton in the acylthiourea moiety on complexation followed by the delocalization of the C=O and C=S π-electrons. Also the peak at 1261 cm^{-1} which was assigned

to C=S stretching vibration reduced to lower frequencies in the metal complexes showing its coordination to the metal center with CuCBEDEA and NiCBEDEA showing 1256 and 1236 cm^{-1} valuesfor C=S stretching vibration respectively. These results are in agreement with literature reports [4,19,27,41]. Also, a new weak band appeared at 1589 cm^{-1} and 1634 cm^{-1} for NiCBEDEA and CuCBEDEA respectively. These were assigned to C=N stretching vibration, showing that there was delocalization of the π-electrons on the thione group to the C-N bond. Thus, it can be concluded that the ligand coordinated via the thione sulfur and the carbonyl oxygen to give a six- membered ring system with the metal atom. Therefore the π-electrons are delocalized between the CO-N-CS moiety during coordination.

In the electronic spectra, CuCBEDEA showed peaks at 28,746 cm^{-1}, 21,435 cm^{-1} and 15,890 cm^{-1} which can be assigned to the $^1A_{1g} \rightarrow E_g$, $^1A_{1g} \rightarrow {}^1B_{1g}$ and $^1A_{1g} \rightarrow {}^1A_{2g}$ transitions of the square planar geometry. Similarly, NiCBEDEA displayed absorption bands at 27,739 cm^{-1}, 20,930 cm^{-1} and 15,235 cm^{-1} which can be assigned to the $^1A_{1g} \rightarrow E_g$, $^1A_{1g} \rightarrow {}^1B_{1g}$ and $^1A_{1g} \rightarrow {}^1A_{2g}$ transitions of the square planar geometry. However, only a few works havebeen reported on the electronic spectra of acylthiourea metal complexes. It has been mentioned that UV spectroscopy does not find extensive use in structure elucidation of thioureas [1]. On the basis of the IR, UV/vis spectra and mass spectra, the structure of the metal complexes was proposed (Figure 5).

3.7. In-vitro antimicrobial assay

The compounds were screened for their antimicrobial activities against 17 bacteria and 4 fungi and were reported based on their inhibition zone diameter and minimum inhibitory concentration as shown in Tables 4 and 5 respectively. The minimum inhibitory concentration (MIC) was determined by reported method [32-35]. Two-fold serial dilutions of the compounds were carried out to determine the MIC, within the concentration range 256 to 0.125 μgmL^{-1}. Cultures were grown at 30 – 37 ^oC (18–20 h) and the final inoculums were approximately $10^6 cfumL^{-1}$. The lowest concentration of the study compounds that resulted in complete inhibition of the microorganisms was represented as MIC (μgmL^{-1}). Similar procedures were done on positive controls. In each case, the test was performed in triplicate and the results were expressed as means.MICs were measured for the compounds that showed appreciable growth inhibition zones; the study was restricted to microorganisms that were affected by the compounds. The result on Table 5 showed that the MIC for CBEDEA against the screened bacteria varied from 32 to 256 $\mu g.mL^{-1}$ and was 32 $\mu g.mL^{-1}$ for yeast, *Candidautilis* ATCC 9950.The MICs for the metal complexes were in the range of 32 - 256 for bacteria and 64 – 128 $\mu g.mL^{-1}$ for yeast. The MIC values suggested that some of the studied compounds showed considerable antimicrobial activity.

CBEDEA and its Ni(II) and Cu(II) complexes demonstrated significant effects against some pathogenic bacteria and yeasts. CBEDEA showed significant antimicrobial activity against *P. aeruginosa* ATCC 35032, *S. marcescens* ATCC 13880, *B. Subtilis* ATCC 6633 and *C. utilis* ATCC 9950; CuCBEDEA revealed considerable antimicrobial effect against*M. luteus* ATCC 9341, *S. pneumoniae* ATCC 27336, *P. aeruginosa*ATCC 35032, *B. subtilis*ATCC 6633, *C. utilis*ATCC 9950 and *C. trophicalis* and

NiCBEDEA registered substantial antimicrobial effect against *S. pneumoniae* ATCC 27336, *P. aeruginosa* ATCC 35032, *S. marcescens*ATCC 13880 and *B. Subtilis* ATCC 6633. CuCBEDEA proved to be the most effective among the compounds tested. However, there was no significant improvement on the antimicrobial activity of CBEDEA on complexation. Also, NiCBEDEA did not show any antimicrobial activity against used yeasts as can be seen in Table 5.

The compounds were found to be more effective against Gram-positive bacteria compared to Gram negative bacteria. The observed trend is similar to an earlier report [46]. This is attributed to the nature of the cell walls of theGram-negative bacteria and Gram-positive bacteria. Gram-negative bacteria are not readily permeated by drugs and dyes because of the protective outer membrane of their cell walls [47], such protective outer membrane is absent in Gram-positive bacteria.

From the result of the antimicrobial screening, it can be concluded that bis(acylthiourea) ligand and its copper complex showed promising antimicrobial properties against some tested bacteria and yeast.

Table 4: Inhibition zone diameter (mm) of the synthesized compounds (1000µg/ml) and the reference antibiotics

Test microorganism	Inhibition zone diameter (mm)										
	Compounds			Reference antibiotics							
	CBEDEA	CuCBEDEA	NiCBEDEA	C30	CN10	TE30	AMP10	OFX5	VA30	CTX30	NS100
Escherichiacoli ATCC 35218	-	-	-	24	21	15	-	28	23	10	NT
Enterobacteraerogenes ATCC 13048	-	-	-	19	20	14	-	19	-	20	NT
*Salmonellatyphimirium*ATCC 14028	-	-	-	17	16	15	8	25	21	13	NT
Micrococcusluteus, ATCC 9341	-	12	-	25	15	26	28	24	14	17	NT
*Stapylococcusaureus*ATCC 25923	8	9	-	23	20	22	20	23	13	12	NT
Stapylococcusepidermidis ATCC 12228	8	9	-	22	17	19	17	22	12	13	NT
Klebsiellapneumoniae ATCC 13882	-	-	-	21	19	20	-	27	23	14	NT
Streptococcuspneumoniae ATCC 27336	10	13	14	24	20	25	14	28	29	15	NT
*Pseudomonasaeruginosa*ATCC 35032	16	12	11	22	20	20	-	29	18	14	NT
Corynebacteriumxerosis ATCC 373	-	-	-	20	17	25	27	22	21	20	NT
*Mycobacteriumsmegmatis*ATCC 607	-	-	-	23	18	26	19	30	20	12	NT
Listeriamonocytogenes ATCC 19112	-	-	-	19	14	12	12	29	25	16	NT
Serratiamarcescens ATCC 13880	12	9	13	23	19	13	19	27	27	13	NT
Proteusvulgaris ATCC 33420	-	-	-	17	24	17	-	26	24	18	NT
Entereococcusfaecalis ATCC29212	-	-	-	16	11	19	14	28	20	16	NT

Bacillluscereus ATCC 11778	-	9	-	23	24	25	-	28	21	17	NT
Bacillussubtilis ATCC 6633	13	18	13	22	20	12	-	27	20	16	NT
Candidaalbicans ATCC 10231	-	8	-	NT	NT	NT	NT	NT	NT	NT	22
Candidautilis ATCC 9950	16	11	-	NT	NT	NT	NT	NT	NT	NT	21
Candidatrophicalis	-	12	-	NT	NT	NT	NT	NT	NT	NT	20
Saccharomycescerevisiae ATCC 9763	-	-	-	NT	NT	NT	NT	NT	NT	NT	15

Key: C30: Chloramphenicol (30 mg Oxoid), CN10: Gentamycin (10 mg Oxoid), TE30: Tetracycline (30 mg Oxoid), E15: Erythromycin (15mg Oxoid), AMP10: Ampicillin (10 mg Oxoid), OFX5: Ofloxacin (5 mg Oxoid), VA30: Vancomycin (30 mg Oxoid),CTX: Cefotaxime (30 mg Oxoid), NS: Nystatin (100 mg Oxoid),
(-): Zonedid not occur. NT: Not tested.

Table 5: Antimicrobial activities reported as the minimum inhibitory concentration (MIC, µg.mL^{-1})

Test Microorganisms	CBEDEA	CuCBEDEA	CuCBEDEA
Micrococcusluteus, ATCC 9341	-	64	-
*StapylococcusaureusA*TCC 25923	256	256	-
Stapylococcusepidermidis ATCC 12228	256	256	-
Pseudomonasaeruginosa ATCC 35032	32	64	128
Klebsiellapneumoniae ATCC 13882	-	-	-
Streptococcuspneumoniae ATCC 27336	128	64	32
Mycobacteriumsmegmatis ATCC 607	-	-	-
*SerratiamarcescensA*TCC 13880	64	256	64
*BacillluscereusA*TCC 11778	-	256	-
*BacillussubtilisA*TCC 6633	64	16	64
Candidaalbicans ATCC 10231	-	256	-
*CandidautilisA*TCC 9950	32	128	-
Candidatrophicalis	-	64	-
Saccharomycescerevisiae ATCC 9763	-	-	-

(-) = No effect

3.8.Analysis of Docking Calculations

The use of computational techniques in the design and development of new chemotherapeutic agent has become a common practice in both academic and industrial field because of their cost and time efficiencies [48,49]. Due to several kinds of literature that proposed compounds of thiourea series to demonstrate antibiotic property, we investigated the possibility of CBEDEA, CuCBEDEA and NiCBEDEA to bind to bacterial β-lactamase [50,51]. Aside from being a validated antibiotic target, the protein was chosen because its production is a significant resistance-mechanism that impedes the function of antibiotics [52]. The theoretical free binding energy retrieved from the highest populated clusters of poses and characterized by the top-ranking score revealed that all the molecules could inhibit the activity of the enzyme. Moreover, metal complexes of CBEDEA showed improved affinity for the protein (CBEDEA = -6.7 kcal/mol, CuCBEDEA = -8.7 kcal/mol and NiCBEDEA = -8.2 kcal/mol).

Thus, the observed increased interaction of CuCBEDEA and NiCBEDEA with the target protein is an advantage. The best dock poses of the compounds identified unique binding mode toward β-lactamase (Figure 6). The decrease in the size of the ligand molecule due to complexation with the metal ion possibly enabled CuCBEDEA and NiCBEDEA to fit more appropriately within the active site groove of the protein. All the candidates had one of their terminal phenyl rings accommodated within the enzyme cavity surrounded by the following amino acids with hydrophobic chains: Val124, Val212, Val214, Leu219 and Ala223. Also, all the compounds made hydrogen bonding interaction with β-lactamase Ser64, Lys67 and Asn152. The observed π-π contact between the aromatic rings of CuCBEDEA and Tyr224, which is absent in others, could account for its increased binding affinity for the protein. The result of the docking simulation shows strong correlation with the in vitro antimicrobial result, with CuCBEDEA showing the highest activity.

4. Conclusion

A new bis(acylthiourea) ligand and its Ni(II) and Cu(II) metallic derivatives were synthesized. The ligand behaved as a dianionictetradentate molecule, coordinating through the thione sulfur and the carbonyl oxygen.Four coordinate square planar geometries have been proposed for the Ni(II) and Co(II) complexes.The results of the electrostatic potential map for the bis(acylthiourea) predicted the possibility of metal coordination through the carbonyl and thione functional groups.Results of non-covalent interation studies revealed the presence of significant hydrogen bonding and other weak non-covalent interaction in the molecule. Docking calculations revealed that the compounds had an affinity for a protein notable for its involvement in the drug resistance mechanism of bacteria – beta-lactamase. Moreover, complexation of the ligand appeared to improve the binding affinity toward the protein and analysis of their binding poses showed that the compounds adopted unique conformations within the binding cavity of the studied protein. Furthermore, *in-vitro* screening of the compounds against Gram-positive bacteria, Gram-negative bacteria and yeast confirmed the antimicrobial

potencies of the candidates. However, observation suggests the metal complexes failed to improve permeability across the bacteria cell walls because almost only the Gram-positive bacteria were susceptible to the compounds. Nonetheless, CuCBEDEA appeared to be most promising compound because it demonstrated lowest theoretical binding affinity towards beta-lactamase and highest antimicrobial activity. Therefore, further attention on the compound is necessary, and the predicted binding poses could guide the structural modification in the activity optimization process.

Acknowledgement

Dr. Christopher J. Ziegler and Briana Schrage' of Department of Chemistry, the University of Akron, 43325, Akron, OH, USA are acknowledged for the collection of the X-ray crystal data.

Appendix A : Supplementary material

CCDC 1819392 contains the supplementary crystallographic data for this paper. These data can be obtained free of charge via http://www.ccdc.cam.ac.uk/conts/retrieving.html (or from the Cambridge Crystallographic Data Centre, 12, Union Road, Cambridge CB2 1EZ, UK; fax: +44 1223 336033). Supplementary data for this publication can be found at….

References

[1] A. Saeed, U. Florke, M.F. Erben, A review on the chemisty, coordination, structure and biological properties of 1-(acyl Iaroyl)-3-(substituted) thioureas. J. Sulfur Chem. 35 (2014) 318-355.
[2] H. Liu, W. Yang, W. Zhou, Y. Xu, J. Xie, M. Li, Crystal structures and antimicrobial activities of copper (II) complexes of fluorine thioureido ligands.Inorg.Chim.Acta 405 (2013) 387-397.
[3] M. Lipowska, B.L. Hayes, L. Hansen, A. Taylor, L.G. Marzilli, Rhenium(v) oxo complexes of novel N2s2 dithiourea (DTU) chelate ligands: synthesis and structural and structural characterization. Inorg. Chem. 35 (1996) 4227-4231.
[4] G. Binzet, H. Arslan, U. Florke, N. Kulcu, N. Duran, Synthesis, characterization and antimicrobial activities of transition metal complexes of N,N-dialkyl-N'-(2-chlorobenzoyl) thiourea derivatives. J. Coord. Chem. 59 (2006) 1395-1406.
[5] E.J. Waheed, Synthesis and characterization of some metals complexes of [N-[(benzoylamino)-thioxomethyl] proline]. J. Al-Nahrain Uni. 15 (2012) 1-10.
[6] Y.F. Yuan, J.T. Wang, M.C. Gimeno, A. Laguna, P.G. Jones, Synthesis and characterization of copper complexes with N-ferrocenoyl-N'(alkyl)thioureas. Inorg.Chim.Acta 324 (2001) 309-317.
[7] T.S. Smith, W. Henderson, B.K. Nicholson,Cycloauratedgold(III) complexes with monoanionic thiourea ligands. Inorg.Chim.Acta 408 (2013) 27-32.
[8] C. Sacht, M.S. Datt, S. Otto, A. Roodt, Chiral and achiral platinum (II) complexes for potential use as chemotherapeutic agents: crystal and molecular structures of cis-[Pt(L')$_2$] and [Pt (L') Cl(MPSO)] [HL'= N,N-diethyl-N'-benzoylthiourea]. J. Chem. Soc. Dalton Trans. 5 (2000) 727-733.
[9] R.L. Zuckerman, R.G. Bergman, Structural factors that influence the course of overall [2+2] cycloaddition reactions between midozirconocene complexes and heterocumulene. Organometallics 19 (2000) 4795-4809.
[10] C.K. Ozer, H. Arslan, D. Van derveer, N. Kulcu, Synthesis and characterization of N-(aryl carbamothioyl).cyclohexanecarboxamide derivatives: the crystal structure of N-(Naphthalen-1-ylcarbamothioyl) cyclohexanecarboxamide. Molecules 14 (2009) 655-666.
[11] P. Byrne, D.R. Turner, G.O. Hoyd, N. Clarke, J.W. Steed,Gradual transition from NH---Pyridylhydrogen bonding to the NH---O tape synthon in pyridyl ureas.Crys.Growth Des. 8 (2008) 3335-3344.
[12] M.W. Hosseinni,Reflection on molecular tectonics. Cryst.Eng. Comm. 6 (2004) 381-322.
[13] P.A. Gale, S.E. Garcia-Garrido, J. Garric, Anion receptors based on Organic frameworks: highlights from 2005 and 2006. Chem. Soc. Rev. 37 (2008) 151-190.
[14] A.G. Doyle, E.N. Jacobsen, Small molecule H-bond donors in asymmertric catalysis. Chem. Rev. 107 (2007) 5713-5743.
[15] M. Behray, C.A. Webster, S. Pereira, P. Ghosh, S. Krishnamurthy, W.T. Al-Jamal, Y. Chao,Synthesis of diagnostic silicon nanoparticles for targeted delivery of thiourea to epidermal growth factor receptor-expressing cancer cells. Appl. Mat. Int. 8 (2016 8908-8917.
[16] H. Peng, Y. Liang, L. Chen, L. Fu, H. Wang, H. He, Efficient synthesis and biological evaluation of 1,3-benzenedicarbonyldithioureas.Biorg. Med. Chem. Let. 21 (2012) 1102 – 1104.

[17] Y. Benabdelouahab, L. Munoz-Moreno, M. Frik, I. Cueva-Alique, M.A. Amrani, M. Contel, A.M. Bajo, T. Cuenca, E. Royo, Bonding and anticancer properties of water-soluble chiral p-cymene Ru(II) compounds with amino-oxime ligands.Euro. J. Inorg. Chem. 13 (2015) 2295-2307.

[18] W. Hernandez, E. Spodine, L. Beyer, U. Schroder, R. Richter, J. Ferreira, N. Pavani, Synthesis, characterization and antitumor activity of copper(II) complexes, [CuL_2] [HL1-3 =N,N-Diethy-N'-(R-benzoyl)thiourea (R=H, o-Cl and p-NO_2].Bioinorg. Chem. App. 3 (2005) 299-316.

[19] M.F. Emen, H. Arslan, N. Kuluc, U. Florke, N. Duran, Synthesis, characterization and antimicrobial activities of some metal complexes with N-(2-chlorobenzoyl)thiourea lignads: the crystal sstructure of fac-[Co L3] and cis-]PdL2]. Pol. J. Chem. 79 (2005) 1615-1626.

[20] S. Saeed, N. Rashid, M. Ali, R. Hussan, P.G. Jones, The crystal strycture of 1-(4-chlorophenyl)-3-(4-methylbenzoyl)thiourea.Euro. J. Chem., 1 (2010) 221-227.

[21] R. del Campo, J.J. Criado, E. Garua, M.R. Hermosa, A. Jimenez-Sanchez, J.L. Manzano, E. Monte, E. Rodriquez-Fernandez, F. Sanz, Thiourea derivatives and their nickel(II) and platinum(II) complexes: antifungal activity. J. Inorg. Biochem. 89 (2002) 74-82.

[22] G.Y. Nagesh, K.M. Raj, B.H.M. Mruthyunjayaswamy, Synthesis, characterization, thermal study and biological evaluation of Cu(II), Ni(II) and Zn(II) complexes of Schiff base ligand containing thiazole moiety. J. Mol. Struct. 1079 (2015) 423-432.

[23] H. Arslan, N. Duran, G. Boreka, C.K. Ozer, C. Akbay,Antimicrobial activity of some thiourea derivatives and their nickel and copper complexes. Molecules 14 (2009) 519-527.

[24] R. Custelcean, M.G. Gorbunova, P.V. Beonnesen, Steric control over hydrogen bonding in crystalline organic solids: a structural study of N,N'-dialkylthioureas. Chem. Euro. J. 11 (2005) 1459-1466.

[25] R. Custelcean, Crystal engineering with urea and thiourea hydrogen-bonding groups. Chem. Comm., 2008 (2007) 295-307.

[26] J.N. Asegbeloyin, E.E. Oyeka, O. Okpareke, A. Ibezim, Synthesis, structure, computational and in-silico anticancer studies of N, N-diethyl-N′-palmitoylthiourea. J. Mol. Struc. 1153 (2018) 69-77.

[27] G. Binzet, N. Kulcu, U. Florke, H. Arslan, Synthesis and characterization of Cu(II) and Ni(II) complexes of some 4-bromo-N-(dialkyl/aryl)carbamothioyl) benzamide derivatives. J. Coord. Chem. 62 (2010) 3454-3462.

[28] M. Frisch, G. Trucks, M. Schlegel, G. Scuseria, M. Robb, J. Cheeseman, G. Scalmani, V. Barone, B. Mennucci, G. Petersson, 2009. Gaussian, Inc., Wallingford CT.

[29] J. Contreras-García, E.R. Johnson, S. Keinan, R. Chaudret, J.P. Piquemal, D.N. Beratan, W. Yang, NCIPLOT: a program for plotting noncovalent interaction regions. J. Chem. Theo. Comput. 7 (2011) 625-632.

[30] C.H. Collins, P.M. Lyne, J.M. Grange, J.O. Falkinham, (2004) Collins and Lyne's microbiological methods. 8. Ed. London: Butterworths, p. 456.

[31] Clinical and Laboratory Standards Institute (2015) M02-A12: performance standards for antimicrobial disk susceptibility tests: approved standard. 12. Ed. Wayne: CLSI, p.1-73.

[32] R.N. Jones, A.L. Barry, T.L. Gavan, J.A. Washington, 1985. Susceptibility tests: microdilution and macrodilution broth procedures. Manual of Clinical Microbiology. 4. Ed. Washington: Am. Soc. Microbio. p. 972-977.
[33] J.H. Jorgensen, M.J. Ferraro, Antimicrobial susceptibility testing: a review of general principles and contemporary practices.J. Med. Microbio., 49 (2009) 1749-1755.
[34] Clinical and Laboratory Standards Institute (2009) M07–A8: Methods for dilution antimicrobial susceptibility testing for bacteria that grow aerobically: approved standard. 8. Ed. Wayne: CLSI, p.1-65.
[35] H.M. Berman, J. Westbrook, Z. Feng, G. Gilliland, T.N. Bhat, H. Weissig, I.N. Shindyalov, P.E. Bourne, The protein data bank, Nucleic Acids Res., 28 (2000) 235e342.
[36] F. Ntie-Kang, J.N. Nwodo, A. Ibezim, C.V. Simoben, B. Karaman, V.F. Ngwa, W. Sippl, M.U. Adikwu, L.M. Mbaze,Molecular modeling of potential anticancer agents from African medicinal plants. J. Chem. Inf. Model 54 (2014) 2433e2450.
[37] W.R.P. Scott, P.H. Hunenberger, I.G. Tironi, A.E. Mark, S.R. Billeter, J. Fennen, A.E. Torda, T. Huber, P. Kruger, W.F. vanGunsteren, The GROMOS biomolecular simulation program package. J. Phys. Chem. 103 (1999) 3596-3607.
[38] A. Saeed, M. Parvez, The crystal strycture of 1-(4-chlorophenyl)-3-(4-methylbenzoyl)thiourea.Cent.Euro. J. Chem. 3 (2005) 780-791.
[39] H. Arslan, U. Flörke, N. Külcü,The crystal and molecular structure of 1-(biphenyl-4-carbonyl)-3-p-tolyl-thiourea.ActaChim.Slov. 51 (2004) 787–792.
[40] G. Kavak, S. Ozbey, G. Binzet, N. Kulcu, Synthesis and single crystal structure analysis of three novel benzoyl thiourea derivatives.Turk. J. Chem. 33 (2009) 867-868.
[41] G. Binzet, G. Kavak, N. Kulcu, S. Ozbey, V. Florke, H. Arslan, Synthesis and characterization of novel thiourea derivatives and their nickel and copper complexes. J. Chem. 2013 (2013) 1-9.
[42] I.G. Csizmadia, Theory and practice of MO calculations on organic molecules, Elsevier.
[43] A. Otero-de-la-Roza, E.R. Johnson, J. Contreras-García, Revealing non-covalent interactions in solids: NCI plots revisited.Phy. Chem. Chem. Phy. 14 (2012) 12165-12172.
[44] Z. Narth, R.A. Maroun, R. Boto, M.L. Chaudret, J.P. Bonnet, J. Piquemal, A. Contreras-García, (2015) Complete NCI perspective: from new bonds to reactivity, in: R.C.C.L.B.S. Esmail Alikhani (Ed.), Applications of Topological Methods in Molecular Chemistry, Springer.
[45] R. Chaudret, B. De Courcy, J. Contreras-Garcia, E. Gloaguen, A. Zehnacker-Rentien, M. Mons, J.P.Piquemal,Unraveling non-covalent interactions within flexible biomolecules: from electron density topology to gas phase spectroscopy. PCCP 16 (2014) 9876-9891.
[46] J.N. Asegbeloyin, O.T. Ujam, E.C. Okafor, I.Babahan, E.P. Coban, A. Ozman, H. Biyik,Synthesis, characterization, and biological activity of N'-[(Z)-(3-methyl-5-oxo-1-phenyl-1,5-dihydro-4H-pyrazol-4-ylidene)(phenyl)methyl]benzohydrazide and its Co(II), Ni(II), and Cu(II) complexes. Bioinorg. Chem. Appl. 2014 (2014) http://dx.doi.org/10.1155/2014/718175.
[47] H. Nikaido, Prevention of drug access to bacterial targets: permeability barriers and active efflux.Science 264 (1994) 382-388.

[48] A. Ibezim, N.J. Nwodo, N. Nnaji, O.T. Ujam, O.O. Olubiyi, C.J. Mbah, In silico investigation of morpholines as novel class of trypanosomaltriosephosphate isomerase inhibitors. Med. Chem. Res. 26 (2016) 180-189.

[49] A. Ibezim, O. Olujide, A. Olubiyi, C.J. Mbah, N.J. Nwodo, Structure-based design of natural products as anti-schistosoma drug: virtual screening, structure activity relationship and molecular dynamic studies.Cur. Comp.-aid. Drug Des. 13 (2017) 91-100.

[50] A. Bielenica, J. Stefanska, K. Stepien, A. Napiorkowska, E. Augustynowicz-Kopec, G. Sanna, S. Madeddu, S. Boi, G. Giliberti, M. Wrzosek, M. Struga, Synthesis, cytotoxicity and antimicrobial activity of thiourea derivatives incorporating 3-(trifluoromethyl)phenyl moiety.Euro. J. Med. Chem. 101 (2015) 111-125.

[51] A.N. AbdHalim, Z. Ngaini, Synthesis and bacteriostatic activities of bis(thiourea) derivatives with variable chain length. J. Chem. 2016 (2016) doi.org/10.1155/2016/2739832.

[52] S. Shaikh, J. Fatima, S. Shakil, S. Mohd, D. Rizvi, M.A. Kamal, Antibiotic resistance and extended spectrum beta-lactamases: types, epidemiology and treatment.Saudi J. Bio. Sci. 22 (2015) 90-101.

Figure captions

Figure 1: Molecular structure of CBEDEA showing the atomic numbering scheme at 30% ellipsoid. a) ORTEP diagram b) showing the zigzag conformation of CBEDEA.

Figure 2: The crystal packing of CBEDEA showing the zig-zag structure of the molecule (dashed lines denote the intramolecular hydrogen bonding)(grey: C, red: O, yellow: S, blue : N, green: Cl. H – atoms were omitted for clarity).

Figure 3: Electrostatic potential map and contour diagram for CBEDEA ligand

Figure 4 : 3D isosurface representation (top) and 2D (bottom) NCI plots for CBEDEA. The 3D isosurface uses a blue-green-red colour scheme from -0.04 a.u.(blue) < sign(λ_2)ρ < +0.04 a.u (red).

Figure5: Proposed structure of Cu(II) and Ni(II) complex of CBEDEA

Figure 6: Predicted binding modes for CBEDEA and its metal complexes toward β-lactamases. Carbon atoms are coloured grey in CBEDEA, pink in CuCBEDEA and green in NiCBEDEA while the rest of the atoms retain in their standard colours. Yellow dash lines represent hydrogen bonding.

a

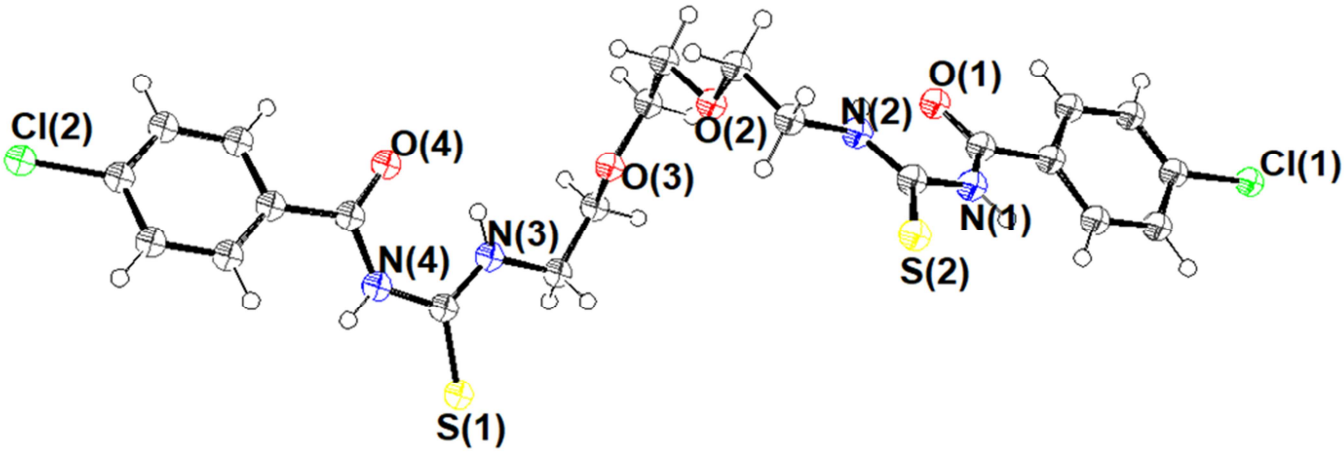

b

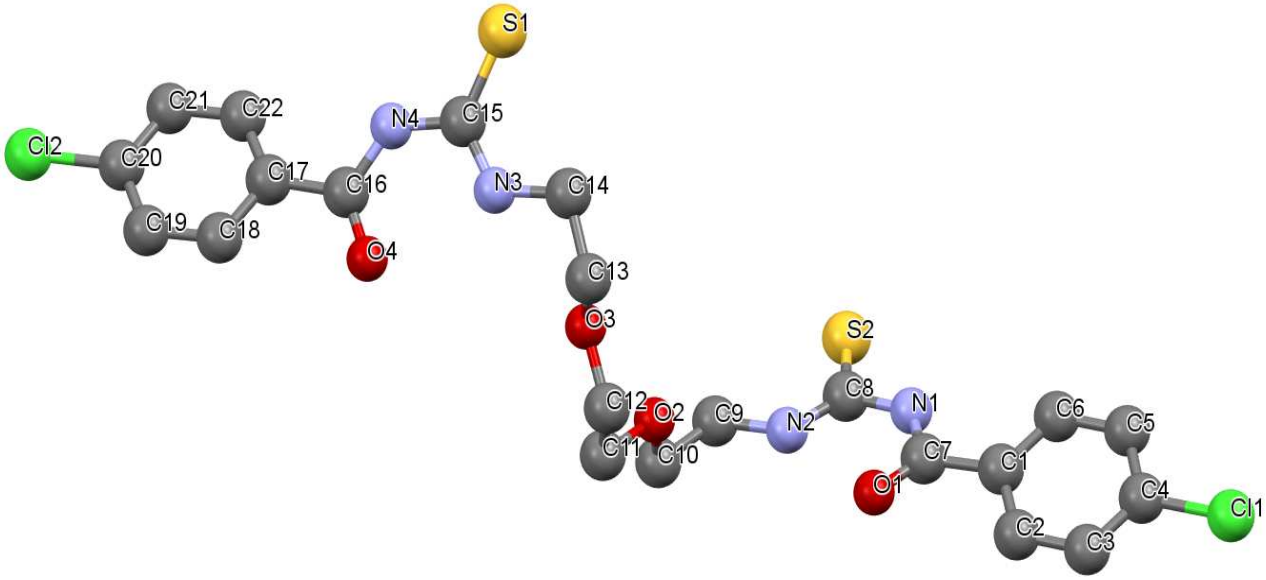

Figure 1: Molecular structure of CBEDEA showing the atomic numbering scheme at 30% ellipsoid. (a) ORTEP diagram (b) showing the zigzag conformation of CBEDEA.

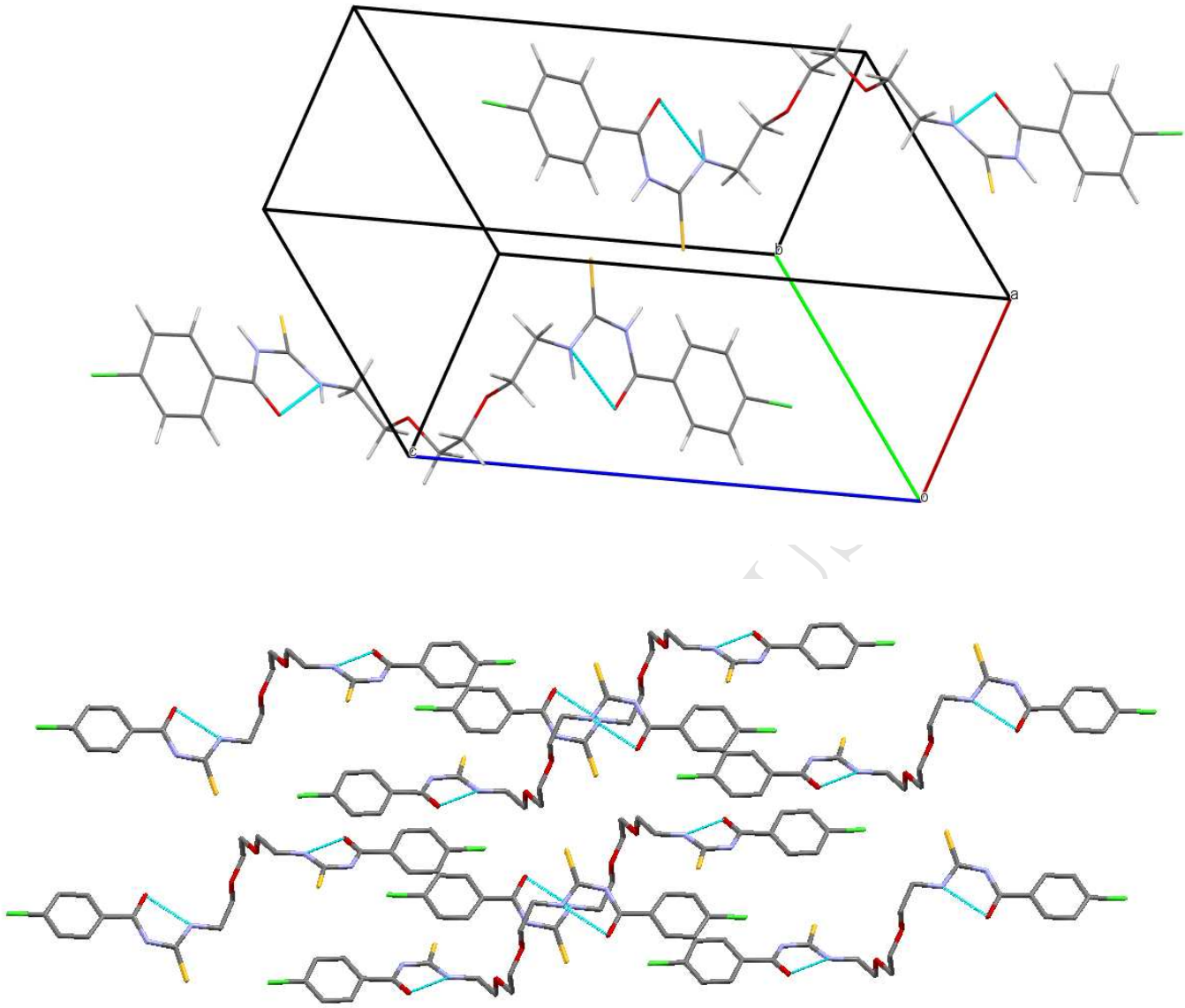

Figure 2: The crystal packing of CBEDEA showing the zig-zag structure of the molecule (dashed lines denote the intramolecular hydrogen bonding)(grey: C, red: O, yellow: S, blue : N, green: Cl. H – atoms were omitted for clarity).

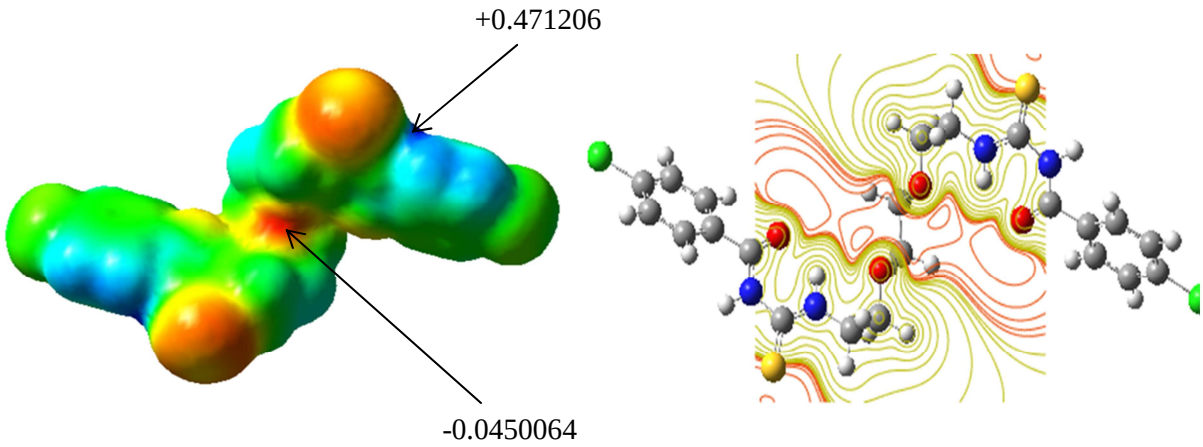

Figure 3: Electrostatic potential map and contour diagram for CBEDEA ligand.

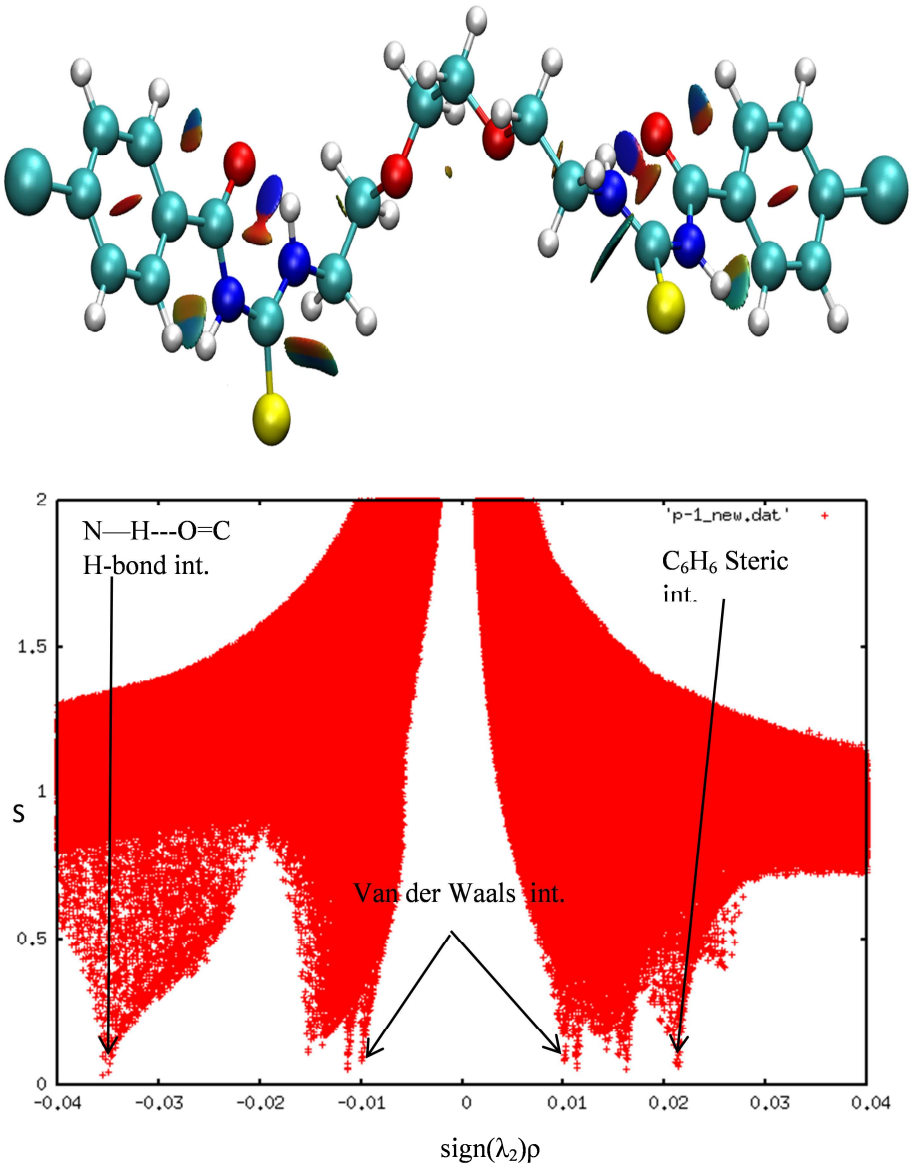

Figure 4 : 3D isosurface representation (top) and 2D (bottom) NCI plots for CBEDEA.

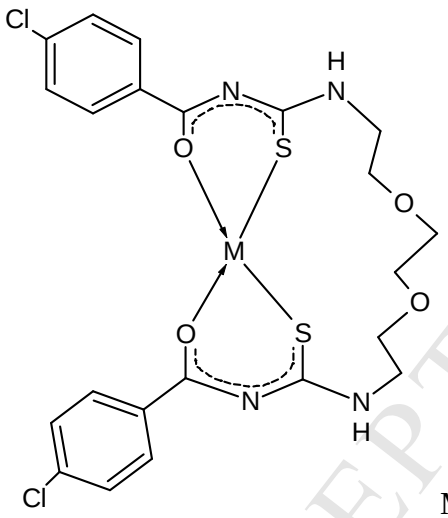

M = Cu or Ni

Figure5: Proposed structure of Cu(II) and Ni(II) complex of CBEDEA.

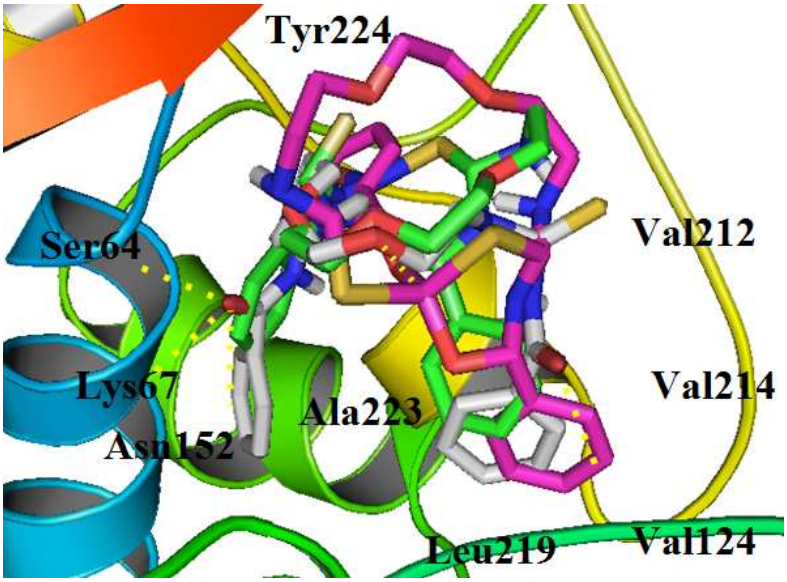

Figure 6: Predicted binding modes for CBEDEA and its metal complexes toward β-lactamases. Carbon atoms are coloured grey in CBEDEA, pink in CuCBEDEA and green in NiCBEDEA while the rest of the atoms retain in their standard colours. Yellow dash lines represent hydrogen bonding.

Highlights

A new hydrogen bonded bis-thiourea ligand has been synthesized and structurally characterised

Electrostatic potential analysis suggests metal chelation through the carbonyl and thione donor groups

Spectroscopic data predicted square planar geometry for the metal complexes

Biological assay revealed higher bioactivity for the Cu complex